

Gravity
Magnetics
and Geology
of the
Guichon Creek Batholith

Bulletin 62

C. A. Ager
W. J. McMillan
T. J. Ulrych

1972

British Columbia Department of Mines and Petroleum Resources

LIBRARY
DEPT. I.A.N.D.
P.O. BOX 1500
YELLOWKNIFE, N.W.T.
CANADA X1A 2R3



TABLE OF CONTENTS

	Page
Introduction	5
Acknowledgments	5
Geology	5
The Gravity Survey	6
Gravity Observations	6
Survey Procedure	6
Elevations	7
Rock Densities	7
Gravity Corrections	7
Data Enhancement Techniques	8
Interpolation of Gravity Map to a Square Grid	8
Filtering of Potential Fields	9
Regional-Residual Separation	9
The Filtered Gravity Maps	9
Arriving at the Initial Model of the Batholith	10
Model of the Batholith	10
Gross Shape	10
The Calculated Gravity Map	11
Summary and Conclusions	11
References	12
Appendix A. Summary of Survey Results	13

TABLE

1. Summary of errors involved in calculating the Bouguer anomaly for each station	8
---	---

FIGURES

1. Simplified geology of the Guichon Creek batholith	In pocket
2. Gravity station location map	In pocket
3. Density map of rocks of the Guichon Creek batholith	In pocket
4. Complete Bouguer anomaly map of the Guichon Creek batholith	In pocket
5a. Selection of cutoff wavenumber (k_c) using vertical prism model	In pocket
5b. Method of separating regional and residual gravity values	In pocket
6. Regional Δg anomaly map derived by filtering from the complete Bouguer anomaly map	In pocket
7. Compilation of geophysical data indicating dips along the edge of the batholith	In pocket

	Page
8. Total aeromagnetic field map of the Guichon Creek batholith derived by digitizing published aeromagnetic maps	In pocket
9. Regional aeromagnetic map of the Guichon Creek batholith derived by filtering the total aeromagnetic field map	In pocket
10. Second vertical derivative aeromagnetic map of the Guichon Creek batholith derived by filtering the total aeromagnetic field map.	In pocket
11a. Calculated gravity map for model of the Guichon Creek batholith	In pocket
11b. Gross shape plan of the Guichon Creek batholith derived from the gravity data	In pocket
12. Depth-gravity section A-A', looking northerly	In pocket
13. Depth-gravity section B-B', looking easterly	In pocket

Gravity, Magnetism, and Geology of the Guichon Creek Batholith

INTRODUCTION

Three gravity profiles were run during the summer of 1971 as an extension of the detailed geological mapping project of the Guichon Creek batholith. Two profiles are oriented east-west; the third is roughly north-south. By blending data from the gravity and geological surveys it was hoped to delineate a reasonable three-dimensional model of the batholith.

ACKNOWLEDGMENTS

We are indebted to the Gravity Division, Earth Physics Branch of the Department of Energy, Mines and Resources, Ottawa, for supplying instrumentation, computer time, and expert advice. In particular, thanks go to Dr. R. A. Stacey, J. B. Boyd, and R. V. Cooper for their unselfish technical support during the course of the survey.

In 1968, Dr. J. M. Carr was instrumental in having a reconnaissance east-west gravity profile run across the Guichon Creek batholith by the Gravity Division of the Department of Energy, Mines and Resources. Detailed coverage of the batholith was planned but not done by the Gravity Division. Subsequently, Dr. A. Sutherland Brown and Dr. W. F. Slawson initiated this project which was financed in large part by the British Columbia Department of Mines and Petroleum Resources.

GEOLOGY

The Guichon Creek batholith is a semiconcordant dome that is elongated slightly west of north. It intrudes sedimentary and volcanic strata of the Permian Cache Creek Group and Upper Triassic Nicola Group and is unconformably overlain by sedimentary and volcanic strata ranging in age from Middle Jurassic to Middle Tertiary. The batholith appears to be bounded on the east and west sides by faults of regional extent.

In plan, Figure 1, the batholith is composed of several nearly concentric phases which have contacts that may be sharp locally but are generally gradational. Extensive K-Ar dating has shown that, within the limits of error, all phases began retaining argon at the same time, 198 ± 8 million years ago (Northcote, 1969). However, geologic data indicate that phases are progressively younger from the border of the batholith inward.

The phases of the batholith are separable on the basis of compositional and textural criteria (McMillan, 1972). From the oldest to the youngest, the following phases are distinguishable:

- (1) The border, HYBRID phase, which ranges widely in composition from a uniform mafic-rich quartz diorite to highly variable mixed rocks. The variation is apparently related to contamination. It is typically rich in mafic minerals.
- (2) The HIGHLAND VALLEY phase which consists of the Guichon and Chataway granodiorites. The Guichon granodiorite has 15 per cent mafic minerals which occur as unevenly distributed clusters of anhedral grains, whereas the Chataway granodiorite has 12 per cent mafic minerals and is characterized by evenly distributed blocky mafic crystals, usually hornblende.
- (3) The BETHLEHEM phase granodiorite has 8 per cent mafic minerals. It is characterized by irregularly distributed coarse-grained poikilitic hornblende crystals in a matrix containing evenly distributed fine to medium-grained mafic crystals.
- (4) The centre of the batholith consists of the BETHSAIDA phase quartz monzonite which has 6 per cent mafic minerals. It is characterized by coarse-grained subhedral quartz phenocrysts and coarse-grained book-like biotite phenocrysts.

A period of extensive dyke emplacement followed the intrusion of the Bethlehem phase and a lesser period followed the Bethsaida phase.

THE GRAVITY SURVEY

GRAVITY OBSERVATIONS: The gravity survey was conducted and the observations reduced according to National Standards as defined by the Gravity Division, Earth Physics Branch, Department of Energy, Mines and Resources, Ottawa, Canada.

The gravity stations were tied into the National Control Network, and can be compared directly to any other observation throughout the Canadian network. The complete Bouguer anomaly values are relative to Ottawa which in turn is tied to the world base point at Potsdam, East Germany. The value at Ottawa is 980,622.00 milligals.

SURVEY PROCEDURE: Three traverses over the central portion of the Guichon Creek batholith were selected on the basis of the mapped geology and the accessibility by four-wheel-drive vehicle. Gravity observations were taken at one-half mile intervals along two east-west and one north-south line (Fig. 2).

For convenience, each station was assigned two numbers:

- (1) *Gravity Division Station Number:* corresponding to the time sequence of observation; 9,000 series for base stations, 19,000 series for detail stations.
- (2) *Grid Point Number:* corresponding to the spatial sequence of each station along individual traverses.

The ground position of each station was marked by a wooden hub on which was nailed an iron cap stamped with the grid point number. The UTM (Universal Transverse Mercator) coordinates for each gravity station were scaled from 1 inch equals 1,320 feet topographic maps covering the survey area. The azimuthal positions were known to an accuracy of ± 150 feet (see Appendix A for a listing).

The gravity observations were made using a Worden Master gravimeter (No. W546) with scale constant 0.39937 milligal per scale division and reading accuracy of 0.10 scale division. Drift control was maintained by tying into a base station network within each four-hour interval.

The base stations were selected at convenient points and tied to each other and to the National network using a LaCoste-Romberg Model G gravimeter. Since this instrument is approximately an order of magnitude more accurate than the Worden and has virtually no instrument drift, observed gravity values, accurate to ± 0.04 milligal were determined for the base network.

ELEVATIONS: The elevations (above mean sea level, MSL) at each station were determined by a level survey supervised by Mr. George New of the British Columbia Department of Lands, Forests, and Water Resources. The elevations, to the top of the wooden hubs, were measured to an accuracy of ± 0.10 foot using a Jena Automatic Level (see Appendix A for details).

ROCK DENSITIES: Rock samples were collected from 85 outcrops along and around the survey routes. Three samples were selected at random from each outcrop. Bulk densities were measured using a Mettler balance. The value assigned to each outcrop was the average of the three samples. These densities were plotted along with over 600 other measurements made by F. Karpick of the Department of Mines and Petroleum Resources on samples from the batholith. The contoured surface density map of the Guichon batholith is shown on Figure 3.

Rock densities generally increase from younger to older rock phases. However, only two major divisions can be made on the basis of density. They are:

- (1) The Hybrid phase and country rocks.
- (2) The Highland Valley, Bethlehem, and Bethsaida phases.

GRAVITY CORRECTIONS

The small variations in observed gravity over a surveyed area include several effects that are unrelated to the geology. Because these variations are of the same order of magnitude as the residual gravity values, it is necessary to compensate for them. The observed gravity values have been corrected for the following effects: Instrument drift, latitude, elevation (Bouguer, free air), and terrain. The Bouguer anomaly map represents the anomalous vertical component of the gravitational acceleration corrected for all these effects. Table 1 lists a summary of errors related to the calculation of each effect, and gives a mean error for the Bouguer anomaly values at each station. The terrain density was taken to be equal to the Bouguer density, 2.67 gm/cm^3 .

Table 1. Summary of errors involved in calculating the Bouguer anomaly for each station

Source of Error	Amount of Error	Range of Error for Survey	Mean Error for Survey*
Observation	±0.1 scale divisions ~ ±0.04 mgal	±0.04 mgal	±0.04 mgal
Latitude	±150 feet ~ ±0.04 mgal	±0.04 mgal	±0.04 mgal
Elevation	±0.10 feet ~ ±0.006 mgal	±0.006 mgal	±0.01 mgal
Terrain	14% of terrain effect	±.17 to ±3.58 mgal	±0.66 mgal
Drift	10% of drift**	±0.001 to ±0.065 mgal	±0.02 mgal

The total mean error for the Bouguer anomalies is therefore ±0.77 mgal.

*Mean error is calculated to nearest .01 mgal.

**Drift corrections were considered to be in error by a maximum of 10 per cent of the effect for each station.

It should be stressed that *the anomalous values are in fact located at the coordinates of the observation stations*. They are not reduced to any datum, but have been corrected for effects down to a datum. The datum chosen for the Guichon Creek batholith was the mean elevation of the observation stations = 4,055 feet. No local continuation of the field was attempted.

DATA ENHANCEMENT TECHNIQUES

INTERPOLATION OF GRAVITY MAP TO A SQUARE GRID: In order to apply standard enhancement techniques, it is necessary that the values be distributed on a regular grid. Therefore, the Δg values at the 205 survey stations together with several regional observations supplied by the Gravity Division were digitized and interpolated to a 1 by 1-mile-square grid using the UBC Xpand Subroutine*. The gridded values of dimension 35 by 46 were then contoured to yield the 'complete Bouguer anomaly map,' Figure 4.

The contours are considered meaningful only near gravity stations. In other regions they represent only an approximation to the anomaly field.

*The value assigned to a grid intersection is set equal to the average of the nearest values in each octant that have been weighted by $1/d$, where d = distance from the data point to the grid intersection.

FILTERING OF POTENTIAL FIELDS: As demonstrated by Fuller (1967), Clarke (1969), and Ulrich (1969), it is convenient to view the enhancement of potential fields as the input-output relation of a linear system. Such an interpretation allows considerable clarification of the effects of a particular enhancement technique by viewing its wavenumber thumbprint. With the advent of the FFT (Fast Fourier Transform), Cooley and Tukey (1965), this approach is now practical.

The choice of the ideal filtering function depends on how one wishes to enhance the data. Common operations on potential fields are vertical continuation, regional-residual separation, and the second derivative computation. A complete set of weighting coefficients together with their frequency images for these operations can be found in Fuller (1967).

REGIONAL-RESIDUAL SEPARATION: The separation of regional (broad scale) from residual (local) anomalies can be viewed as the convolution of the input map with a low pass filter, where the cutoff wavenumbers may be determined by the geology of the region.

By inspection of the surface geology of the Guichon Creek batholith, the minimum horizontal dimension of any major phase of the batholith was taken to be 2 miles. For a vertical prism, this corresponds to a Δg half-width of about 2 miles, Figure 5a. Using this distance as one half a wavelength, the maximum cutoff wavenumber k_c for the batholith was calculated to be 0.25 cycle per mile.

Applying the same reasoning to the maximum dimension of the batholith (36 miles), we calculated a minimum cutoff wavenumber of 1/72 cycle per mile. However, in this case, since it is impractical to build a short filter with a steep leading edge which cuts off at 1/72 cpm, the minimum cutoff wavenumber was set at 0 cpm. Close scrutiny of the regional Δg map edges reveals little large-scale trend, except to the east and southeast where the field is known to overlap with neighbouring sources (for example, Nicola batholith). Therefore this 0 cpm assumption appears justified.

A pictorial representation of the regional-residual separation in the wavenumber domain is shown on Figure 5b.

THE FILTERED GRAVITY MAPS: All filtering operations were performed in the space domain by convolving the input map with the approximate weighting function. The plots of the filtered maps exclude the edge effect of $(L-1)$ points, where L is the filter length.

Because the dimensions of the Δg map were small, 35 by 46, care was taken to select filter operators that were short in length and that attenuated high frequencies (near surface effects) but were still a good approximation to the ideal operator at low wavenumbers. The regional Δg filtered map is presented on Figure 6.

ARRIVING AT THE INITIAL MODEL OF THE BATHOLITH

Two lines of approach were used to define the initial model tested against the results of the gravity survey. The first line was geological, the second geophysical. Based on surface geology and flow foliations, rough east-west and north-south geological profiles were suggested. From the half-width gravity profile and by considering the second vertical derivative, it was possible to estimate the sense and approximate dip of the contact of the Hybrid phase with younger phases of the batholith (Fig. 7).

- (1) The Hybrid phase and older country rock can be treated as a single density unit.
- (2) The grouped Highland Valley, Bethlehem, and Bethsaida phases can also be treated as a single density unit.
- (3) The density contrast between these two units ranges between $-.10$ and $-.15$ gm/cm³.

In order to gain further insight into the subsurface nature of the batholith, published 1-mile-scale aeromagnetic maps of the batholith were digitized at 1 by 1-mile intervals over an area of 68 miles by 45 miles. The resulting total aeromagnetic field map and derived regional and second vertical derivative aeromagnetic maps are presented on these maps but no attempt to interpret them will be made.

The data these maps yield which is pertinent to the gravity model are as follows:

- (1) A halo of magnetic highs partially encloses the grouped younger phases (*see also* Fig. 9).
- (2) The 'highs' suggest that the batholith can be considered as a dipolar source. If this is true, then it is relatively shallow. The highs to the west have higher magnitude, therefore, the batholith probably deepens to the east.
- (3) The zero trace of the second derivative also suggests that the Hybrid and younger phases are magnetically distinct.

From the geological and geophysical data, the batholith is envisaged to be a funnel-shaped body with contacts that dip steeply eastward on the east and west edges, steeply northward on the south edge, and vertically on the north edge. The contact of the east edge changes to a moderate westward dip at depth (Fig. 7).

After computations were begun, the shape of the model was adjusted until a root mean square error *along the traverse lines* of less than 0.9 milligal was obtained for the 205 gravity stations actually observed.

MODEL OF THE BATHOLITH

GROSS SHAPE: All attempts to build a model with density contrast greater than -0.12 gm/cm³ failed to fit the gravity map with the necessary sharpness of detail. Density models with contrasts of $-.13$ and $-.15$ gm/cm³ which give a good fit to the gravity data are shown on Figures 12 and 13. Both models suggest that the batholith is a flattened funnel-shaped body. The spout of the funnel underlies Highland Valley and it plunges at about 80 degrees toward the northeast. The average depth is about 6 kilometres, except in the central core where the depth is more than 12 kilometres.

If one assumes an initial symmetric shape for the batholith, then the pole of the axis of symmetry would plot on the surface at coordinates 120 degrees 57.0 minutes west, 50 degrees 19.0 minutes north with a plunge of 80 degrees toward north 64 degrees east, as shown on Figure 11b. This may be taken as support for the hypothesis that the batholith has been tilted to the west-southwest.

THE CALCULATED GRAVITY MAP: The calculated gravity map for the batholith model is shown on Figure 11a. Care was taken to fit the data along gravity traverses. In other areas, especially peripheral to the batholith source and where observations are sparse, the model represents only an estimate.

In the central region, the -30 -milligal contour could only be approximated. In order to obtain a better fit, the addition of a near surface source is required. This discrepancy may be caused by thick overburden in the valley of Witches Brook. This feature is of little importance to calculating the gross shape of the batholith.

The large inflection in gravity contours to the north can be attributed to the anomaly caused by the overlying Kamloops volcanic rocks. To include this effect, the outcrop trace of the Kamloops Group was approximated by a 12-sided vertical prism and its gravity effect calculated as before and included in the computed Δg map. The density of the volcanic rocks was estimated from measurements on collected rock samples to be 2.60 gm/cm^3 . The average depth of the group was found by trial and error to be about 1 kilometre (see Fig. 11b).

Calculated and observed (regional) gravity anomalies together with depth profiles for sections A-A' and B-B' are shown on Figures 12 and 13. Along these lines the fit is extremely good as evidenced by the comparison of the computed points with the actual Δg values. The fit of the north end of section B-B' could be improved by thinning the Kamloops volcanic cover near B. The discrepancy between regional and calculated Δg at the south end of B-B' is probably a result of interference caused by the Coyle granite which outcrops south of B'.

SUMMARY AND CONCLUSIONS

It is important to realize that the gravity anomalies are in fact located at the coordinates of the observation station. They are not reduced to any datum, but have been corrected for effects down to a datum. It is therefore clear that the anomaly values are located on an irregular surface, and any mathematical treatment of the data must consider this point. This is of special importance in mountainous regions.

The use of linear filter operators on potential fields greatly enhances the interpretation of the data and provides a useful means of anomaly separation. This is most clearly evident on the filtered magnetic map (Fig. 9) where regional magnetic features are highly resolved.

Another use of filtering is to define the second vertical derivative gravity map from which the configuration of the boundary of the source may be inferred (Fig. 7). In particular, the second derivative map suggests that the batholith terminates with a vertical contact to the north, where it underlies the Kamloops volcanic rocks.

On the basis of the gravity and density data, only two subdivisions of the batholith can be made:

- (1) The Hybrid phase and country rock, and
- (2) The Highland Valley, Bethlehem, and Bethsaida phases.

An estimate of the average depth of the Kamloops volcanic rocks overlying the north edge of the batholith was made from the regional Δg map. Using $\rho = 2.60 \text{ gm/cm}^3$, a depth of 1.0 kilometre was determined.

Interpretation of the gravity data led to a density model for the batholith. Its gross shape can be likened to that of a flattened funnel-like structure. The axis of symmetry for the model is tilted about 10 degrees from the vertical and plunges in an east-northeast direction. The maximum depth of the central core is more than 12 kilometres.

Probably the most important result of this study in terms of ore search is shown on Figure 11b. Here there is a striking correlation between the location of large-scale mineral deposits and the surface projection of the root zone of the batholith (Figs. 11b, 12, and 13).

REFERENCES

- Ager, C. A. (1972): A gravity model for the Guichon Creek batholith, unpublished M.Sc. thesis, *U.B.C.*, Geophysics Department.
- Clarke, Garry K.C. (1969): Optimum second derivative and downward continuation filters, *Soc. of Explor. Geophysicists*, Geophysics, Vol. 34, No. 3, pp. 424-437.
- Cooley, J. W. and Tukey, J. W. (1965): An algorithm for the machine calculation of complex Fourier series, *Math. of Computation*, Vol. 19, pp. 297-301.
- Fuller, Brent D. (1967): Two Dimensional Frequency Analysis and Design of Grid Operators, *Soc. of Explor. Geophysicists*, Mining Geophysics, Vol. 2, pp. 658-708.
- McMillan, W. J. (1971): Preliminary Geological Map of Highland Valley, *B.C. Dept. of Mines & Pet. Res.*, Preliminary Map No. 7, 4 sheets.
- (1972): Highland Valley Porphyry Copper District, *International Geologic Congress*, Guidebook, XXIV Session, C. S. Ney and A. Sutherland Brown, editors, pp. 64-82.
- Northcote, K. E. (1969): Geology and Geochronology of the Guichon Creek Batholith, *B.C. Dept. of Mines & Pet. Res.*, Bull. No. 56.
- Ulrych, T. J. (1969): Wavenumber domain analysis and design of potential field filters, Proceedings of a Symposium on decision-making in mineral exploration II, *U.B.C.*

APPENDIX A. SUMMARY OF SURVEY RESULTS

GRID POINT NO.	GRAVITY STATION NO.	UTM COORDINATES ZONE 10 (METRES)		ELEVATION (FEET)	OBSERVED GRAVITY g_o (MGAL)	COMPLETE B. ANOMALY Δg (MGAL)
		EASTING	NORTHING			
0	19570	620800	5603560	940.8	980946.75	-110.16
1B	19694	621590	5603375	1652.2	980910.17	-106.02
2	19693	622325	5603180	2324.8	980872.90	-107.42
3	19568	623100	5603025	2672.3	980854.73	-105.28
4	19567	624050	5602740	2999.9	980835.84	-103.90
5	19566	624840	5602600	3323.5	980819.38	-104.11
6	19628	625590	5602450	3803.9	980791.56	-101.93
7	19565	626300	5602300	3885.7	980787.31	-103.43
8	9251	627100	5602450	4064.2	980776.03	-104.21
9	19501	627930	5602425	4052.4	980773.03	-108.24
10	19502	628740	5602525	3976.1	980775.15	-111.16
11	19503	629550	5602550	3862.0	980780.38	-112.24
12	19504	630350	5602540	3840.0	980780.37	-114.30
13	19505	631075	5602500	3811.1	980781.21	-115.21
14	19506	631925	5602200	3836.1	980776.74	-117.42
15	19507	632700	5601275	3794.6	980774.38	-122.26
16A	19508	633175	5600900	3848.1	980769.23	-122.64
17	19510	634325	5600350	3836.1	980764.55	-127.89
18	19511	635100	5600150	3889.9	980758.75	-130.39
19	19512	635900	5599660	3883.9	980755.87	-133.33
20	19513	636650	5598975	3891.0	980751.84	-134.81
21	19514	637475	5598200	3947.9	980745.37	-137.52
22	19515	638300	5596650	3974.5	980740.10	-141.16
23	19516	639200	5594250	3988.2	980733.39	-146.11
24	19517	640075	5594010	3969.7	980732.51	-148.88
25	19518	640800	5593750	3957.2	980733.66	-148.22
26	9252	641690	5593450	3940.1	980732.14	-150.51
27	19519	642500	5593475	3929.4	980731.74	-151.45
28	19520	643225	5593550	3942.1	980732.56	-149.31
29	19521	644025	5593200	3932.1	980733.26	-149.36
30	19522	644850	5592950	3921.7	980734.76	-148.41
31	19523	645600	5592400	3912.1	980733.64	-150.07
32	19524	646425	5592390	3912.7	980734.63	-149.27
33	19525	647225	5592000	3865.4	980738.28	-148.01
34	19526	648000	5591950	3842.8	980741.74	-145.80
35	19527	648825	5592025	3841.5	980743.49	-144.45
36	19528	649575	5592275	3828.2	980746.58	-142.05
37	19529	650075	5593650	3805.6	980753.34	-136.31
38	19530	651080	5594725	3696.0	980763.30	-134.19
39	19531	651890	5595500	3558.5	980773.96	-126.36

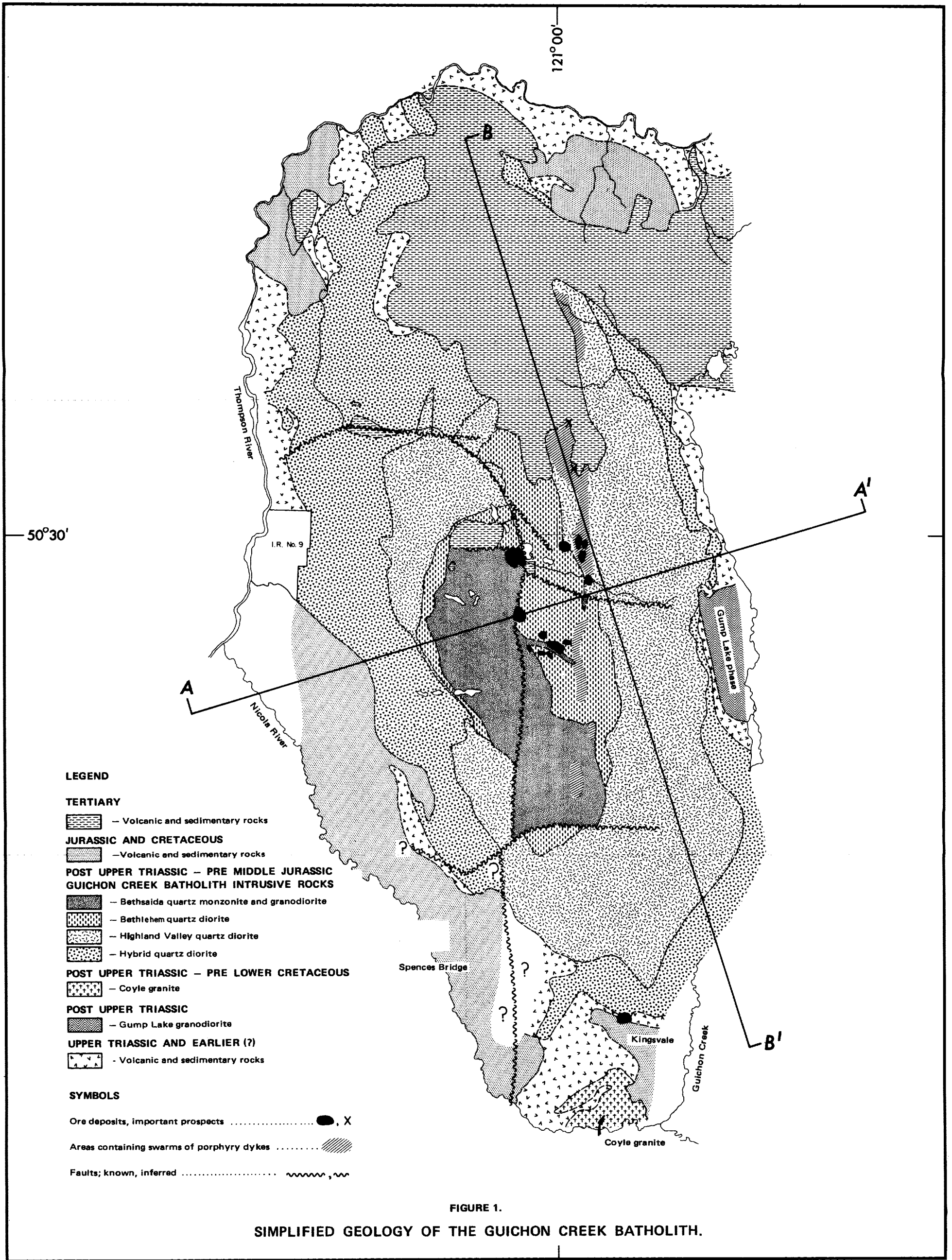
GRID POINT NO.	GRAVITY STATION NO.	UTM COORDINATES ZONE 10 (METRES)		ELEVATION (FEET)	OBSERVED GRAVITY g_o (MGAL)	COMPLETE B. ANOMALY Δg (MGAL)
		EASTING	NORTHING			
40	19532	652650	5595725	3425.2	980782.43	-130.30
41	19533	653525	5595150	3366.5	980785.30	-132.44
42	9253	654225	5595050	3391.2	980785.83	-130.66
43	19534	655000	5595250	3562.0	980780.95	-124.60
44	19535	655700	5596100	3615.8	980780.98	-123.76
45	19536	656500	5595975	3688.9	980780.10	-119.99
46	19537	657325	5596000	3727.9	980780.33	-115.00
47	19538	658175	5595525	3782.5	980777.53	-114.72
48	19539	659050	5595250	3795.0	980776.33	-116.24
49	19540	659900	5595150	3880.0	980772.09	---
50	19541	660675	5594925	3857.9	980774.00	---
51	19542	661470	5594835	3908.0	980771.92	---
52	19543	662350	5594150	3913.8	980772.10	---
53	19601	619575	5587025	748.8	980935.94	-120.15
54	19602	620450	5586100	769.6	980930.46	-118.84
55	19603	621200	5585800	1169.3	980910.07	-109.55
56	19604	622000	5586100	1998.1	980864.46	-118.59
57	19605	622800	5587500	3321.6	980791.14	-117.82
58	19606	623625	5586425	3455.9	980782.91	-113.91
59	19607	624400	5586925	3814.2	980763.17	-116.01
60	19608	625100	5586750	4072.3	980747.01	-119.24
61	19609	625900	5586800	4229.8	980736.88	-118.53
62	19610	626675	5586775	4364.8	980727.48	-121.16
63	19611	627710	5586050	4735.3	980701.54	-122.66
64	19612	628375	5585425	4802.6	980697.80	-123.93
65	19613	629000	5585475	4737.1	980702.82	-123.57
66	19614	629825	5584650	4794.5	980700.95	-121.07
67	19615	630625	5584350	4847.1	980701.38	-118.01
68	19616	631450	5584625	4860.8	980701.41	-118.18
69	19617	632225	5584775	4933.0	980696.54	-118.44
70	19618	633025	5584700	4956.9	980694.10	-120.64
71	19619	633850	5584725	4982.6	980690.82	-122.18
72	9255	634575	5585025	5030.8	980683.43	-127.17
73	19620	635420	5585210	5103.5	980674.35	-130.39
74	19621	636200	5585300	5095.2	980671.81	-133.18
75	19622	637000	5585425	5132.1	980667.72	-136.74
76	19623	637825	5585875	5145.2	980664.97	-139.81
77	19624	638625	5595975	5282.6	980654.87	-141.30
78	19625	639375	5586125	5318.9	980651.62	-143.06
79	19626	640125	5585350	5334.8	980649.61	-141.18
80	19627	640950	5585150	5451.2	980641.54	-143.21
81	19593	641775	5588000	5399.6	980644.29	-144.02
82	19594	642500	5587056	5633.2	980629.04	-144.00

GRID POINT	GRAVITY STATION	UTM COORDINATES ZONE 10 (METRES)		ELEVATION	OBSERVED GRAVITY g_0	COMPLETE B. ANOMALY Δg
NO.	NO.	EASTING	NORTHING	(FEET)	(MGAL)	(MGAL)
83	19596	643300	5587050	5754.7	980620.84	-145.24
84	19600	644100	5586825	5489.6	980637.17	-143.47
85	19599	644875	5586700	5310.0	980648.33	-145.32
86	19598	645550	5586425	5189.0	980655.85	-146.78
87	19685	646475	5584050	5129.0	980658.22	-146.14
88	19684	647275	5583700	4921.5	980671.24	-147.64
89	19683	648125	5583125	4858.2	980675.00	-144.91
90	19680	648875	5584100	4834.4	980677.80	-143.38
91	19681	649625	5584450	4704.8	980686.61	-142.63
92	19682	650375	5584600	4578.6	980695.22	-142.41
93	19679	651200	5587100	4490.0	980704.67	-136.62
94	19678	651950	5587050	4275.8	980719.17	-137.93
95	19677	652925	5587025	4125.6	980729.13	-136.02
96	19676	653250	5587025	4063.0	980732.57	-131.33
97	19675	654325	5586625	3582.9	980761.74	-132.16
98	19674	655125	5586075	3227.3	980782.40	-133.69
99	9254	655925	5585650	3189.5	980786.68	-129.32
100	19669	656850	5581050	3323.7	980776.09	-129.71
101	19670	657675	5581500	3621.6	980763.20	-126.55
102	19671	658450	5581825	3916.1	980748.19	-124.68
103	19672	659175	5581950	4102.1	980737.44	-122.77
104	19673	659975	5581375	4190.9	980730.90	---
105	19695	660700	5580825	4366.0	980719.95	---
106	19696	661425	5580475	4286.0	980723.62	---
107	19629	651550	5557400	1916.6	980838.89	-131.68
108	19630	651825	5558275	1981.4	980833.11	-136.61
109	19631	651775	5559100	2027.3	980831.07	-136.61
110	19632	652050	5559900	2085.1	980827.11	-137.34
111	19633	652075	5560675	2135.1	980824.36	-137.66
112	19634	651850	5561325	2286.4	980817.52	-133.40
113	19635	651550	5562050	2291.9	980819.40	-130.41
114	19636	650775	5562950	2317.2	980822.07	-125.83
115	19637	651150	5563725	2610.9	980804.70	-129.70
116	19638	651525	5564375	2789.0	980796.48	-128.90
117	19639	651825	5565350	2930.2	980789.96	-128.19
118	19640	651400	5566100	3097.2	980783.01	-124.36
119	19641	651375	5566875	3275.0	980772.70	-126.33
120	19642	651725	5567725	3285.6	980773.67	-125.85
121	19643	651950	5568500	3270.7	980773.04	-122.78
122	19644	652175	5569300	3288.3	980771.62	-124.46
123	19645	652450	5570075	3306.3	980768.65	-131.19
124	19646	652650	5570875	3317.5	980770.33	-127.63

GRID POINT NO.	GRAVITY STATION NO.	UTM COORDINATES ZONE 10 (METRES)		ELEVATION (FEET)	OBSERVED GRAVITY g_o (MGAL)	COMPLETE B. ANOMALY Δg (MGAL)
		EASTING	NORTHING			
125	19647	652750	5571675	3346.5	980766.88	-132.14
126A	19648	651775	5572425	3730.3	980742.22	-132.75
126B	19649	650825	5572025	4135.4	980717.90	-131.02
126C	19650	650000	5571900	4241.4	980712.36	-134.62
126D	19651	649200	5572175	4398.9	980703.43	-132.85
126E	19652	648375	5572325	4379.7	980705.00	-134.64
127	19653	647375	5573175	4403.1	980703.26	-135.03
128	19654	647250	5573950	4416.2	980701.91	-137.36
129	19655	647275	5574725	4423.9	980700.89	-135.19
130	19656	647275	5575500	4340.3	980705.49	-139.18
131	19657	647375	5576275	4185.9	980713.88	-138.26
132	19658	647700	5577075	4271.2	980707.71	-141.43
133	19659	647675	5577900	4383.1	980699.90	-140.67
134	19660	647475	5578625	4430.2	980697.43	-142.62
135	19661	647375	5579400	4481.9	980693.73	-142.46
136	19663	647775	5580200	4524.6	980691.59	-140.75
137	19662	648025	5580975	4614.9	980687.23	-142.70
138A	19664	648175	5581775	4647.6	980686.30	-142.94
138B	19665	647050	5581775	4850.4	980673.58	-143.30
139	19666	646400	5582500	5097.7	980658.90	-144.03
140	19667	646100	5583300	5165.3	980655.64	-145.73
141	19668	645950	5584100	5178.8	980655.01	-145.39
142	9259	645575	5584875	5213.2	980653.35	-146.04
143	19597	645550	5585700	5196.1	980654.74	-146.14
144	19598	644875	5586700	5189.0	980655.85	-146.53
145	19595	643875	5587250	5670.4	980626.09	-144.12
146	19593	641775	5588000	5399.6	980644.29	-144.02
147	19592	641875	5588800	5195.2	980657.19	-144.72
148	19591	642200	5589625	5121.6	980661.63	-145.14
149	19590	642775	5590425	4825.8	980679.20	-144.66
150	19589	642975	5591125	4522.9	980697.45	-144.88
151	19588	642600	5591900	4172.7	980719.37	-147.46
152	19587	641075	5592825	4158.8	980722.06	-145.93
153	9252	641690	5593450	3940.1	980732.14	-150.51
154	19572	641350	5594325	4001.9	980731.46	-147.03
155	19573	640750	5595050	4097.7	980728.47	-145.18
156	19574	640500	5595850	4222.6	980722.85	-145.11
157	19575	640775	5596675	4470.5	980709.48	-142.87
158	19576	641050	5597425	4612.5	980702.70	-141.49
159	19577	641275	5598250	4782.7	980693.69	-139.79
160	19578	641925	5599025	4878.8	980690.22	-139.87
161	19579	642025	5599850	5083.3	980679.97	-133.96

GRID POINT NO.	GRAVITY STATION NO.	UTM COORDINATES ZONE 10 (METRES)		ELEVATION (FEET)	OBSERVED GRAVITY g_0 (MGAL)	COMPLETE B. ANOMALY Δg (MGAL)
		EASTING	NORTHING			
162	19580	641300	5600600	5568.2	980649.96	-134.99
163	19581	641175	5601375	5737.6	980641.38	-135.21
164	19582	640825	5602175	5972.9	980628.25	-136.82
165	19583	640700	5602975	5832.2	980637.52	-135.95
166	19584	640075	5603725	5933.5	980627.75	-138.75
167	19585	639200	5604500	5929.5	980631.46	-135.54
168	19586	640075	5605350	5923.4	980633.30	-133.59
169	19692	640300	5606125	5797.0	980642.94	-135.71
170	19691	640275	5606925	5524.5	980661.21	-134.85
171	19690	640225	5607750	5194.9	980682.16	-133.96
172	19689	640250	5608510	5094.3	980689.54	-131.92
173	19688	640275	5609300	4944.9	980700.23	-129.21
174	19564	639730	5610100	4921.6	980703.61	-129.70
175	19687	639650	5610800	4860.7	980710.51	-127.84
176	19686	639510	5611625	4643.8	980728.82	-123.49
177	19563	640225	5612480	4323.7	980751.79	-119.48
178	19562	639675	5613250	4394.1	980748.18	-122.53
179	19561	638150	5613975	4377.5	980747.08	-125.11
180	19560	637990	5614710	4339.6	980751.69	-122.30
181	19559	636480	5615510	4201.9	980762.80	-121.14
182	19558	635200	5616260	4149.1	980767.00	-118.86
183	9257	634425	5617175	4186.9	980767.39	-117.18
184	19557	633950	5617850	4086.9	980775.44	-117.68
185	19556	633975	5618660	3942.4	980783.05	-118.75
186	19555	634000	5619425	3774.8	980792.98	-119.56
187	19554	633700	5620280	3483.7	980814.44	-113.69
188	19552	632900	5620940	3459.1	980817.02	-113.70
189A	19553	632725	5621630	3239.4	980832.34	-112.14
189B	19551	633425	5611730	3120.7	980838.78	-112.73
190	19550	633950	5612550	2930.6	980850.55	-113.99
191A	19549	634575	5623325	3145.0	980837.52	-113.63
191B	19548	635790	5623360	2700.1	980863.29	-113.35
192	19544	635625	5624225	2319.4	980887.78	-110.95
193	19545	634975	5624975	2311.7	980889.88	-110.82
194	19546	634125	5625750	1983.5	980911.64	-108.93
195	19547	633325	5626500	1408.9	980944.46	-107.28

Printed by K. M. MACDONALD, Printer to the Queen's Most Excellent Majesty
in right of the Province of British Columbia,
1972



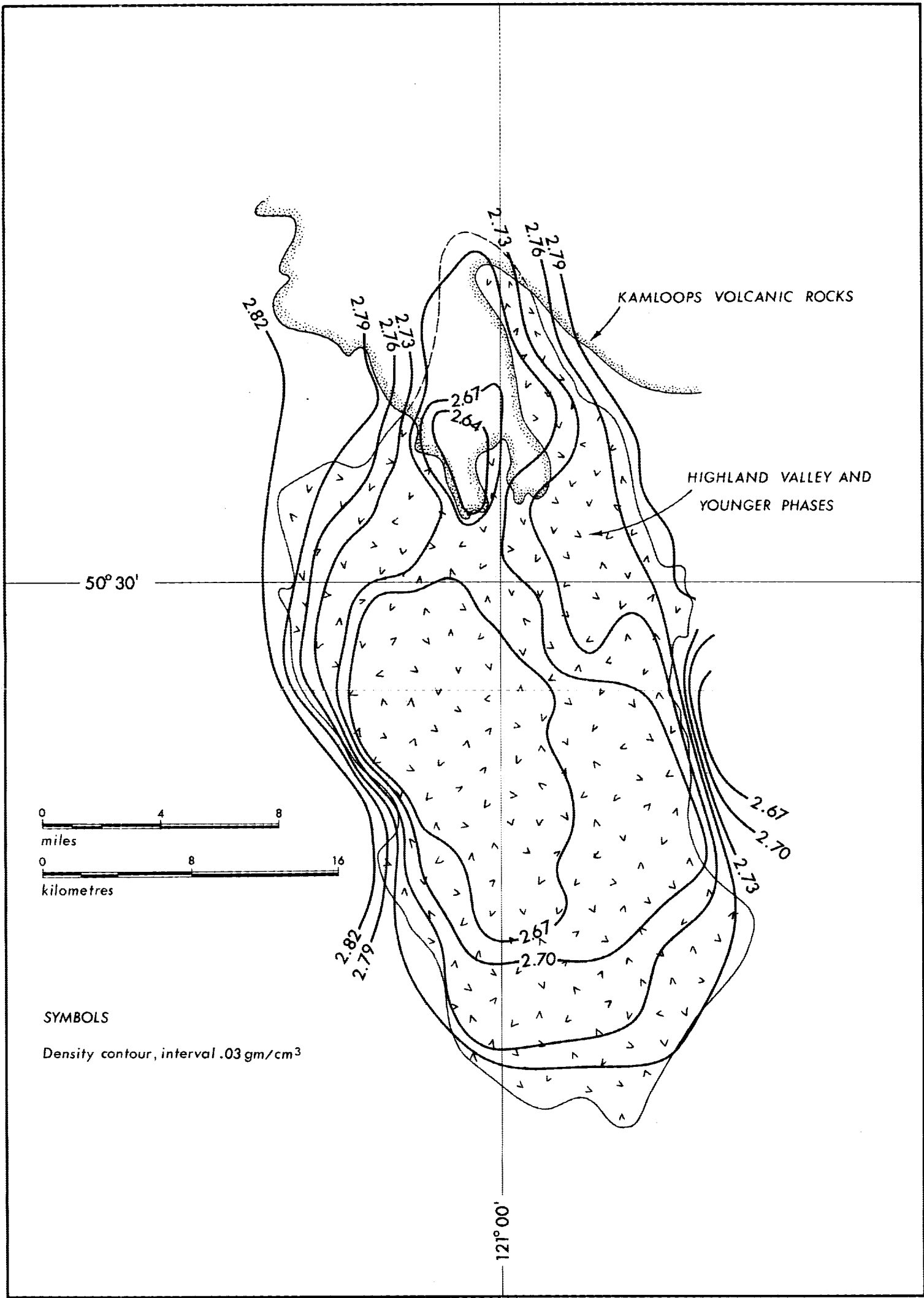


FIGURE 3.

DENSITY MAP OF ROCKS OF THE GUICHON CREEK BATHOLITH.

FIGURE 4.

COMPLETE BOUGUER ANOMALY MAP OF THE GUICHON CREEK BATHOLITH.

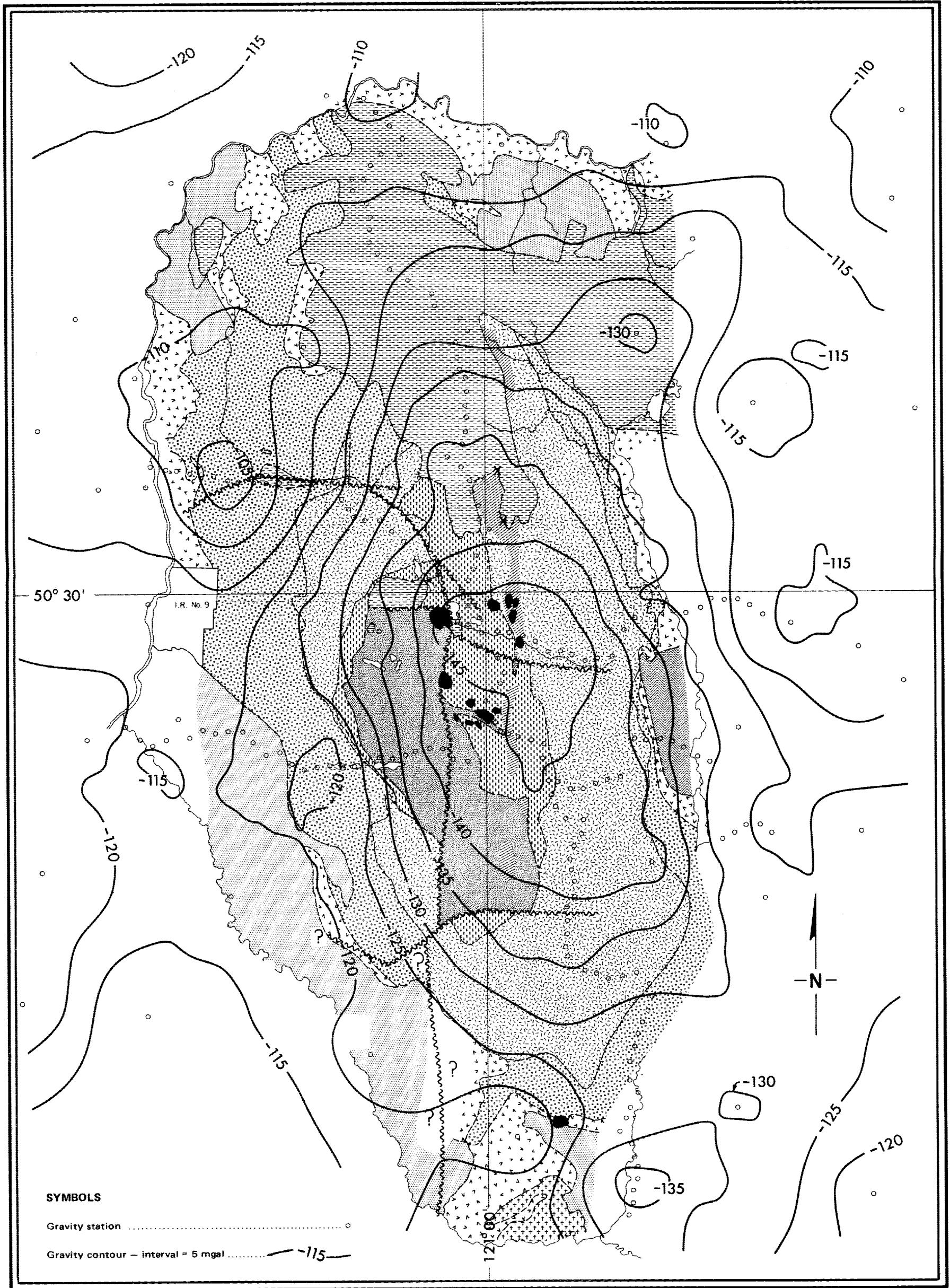
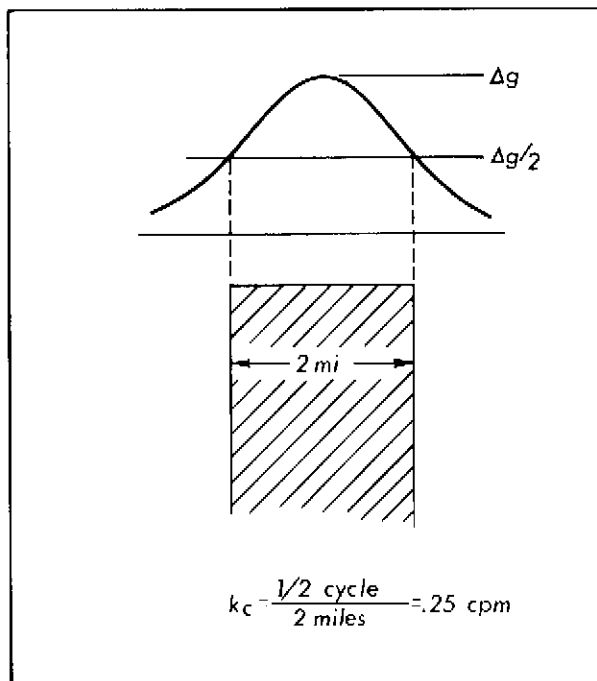
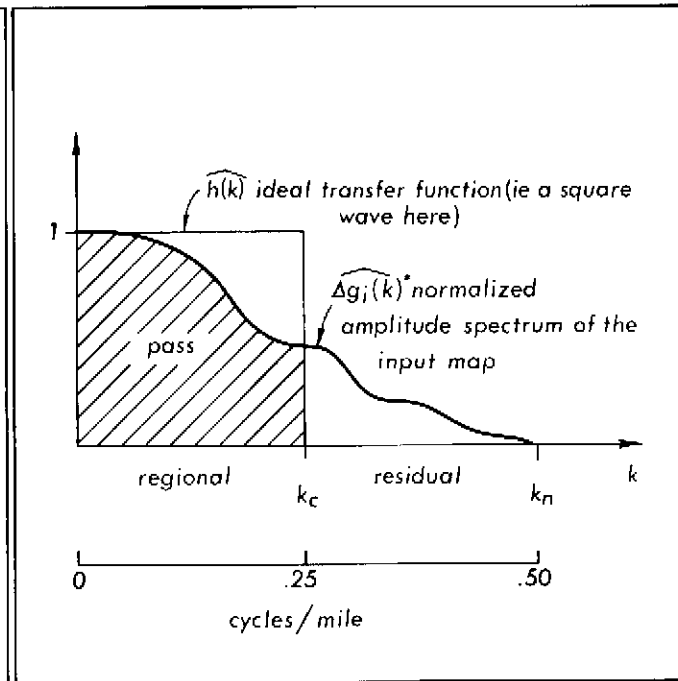


FIGURE 5(a).
SELECTION OF CUTOFF WAVENUMBER (k_c)
USING VERTICAL PRISM MODEL



Space domain

FIGURE 5(b).
METHOD OF SEPARATING REGIONAL
AND RESIDUAL GRAVITY VALUES



Wave number domain

$\widehat{\Delta g_j} = \text{Fourier transform } (\Delta g_j) \dots \text{ note that amplitude only,}$
not phase, is considered

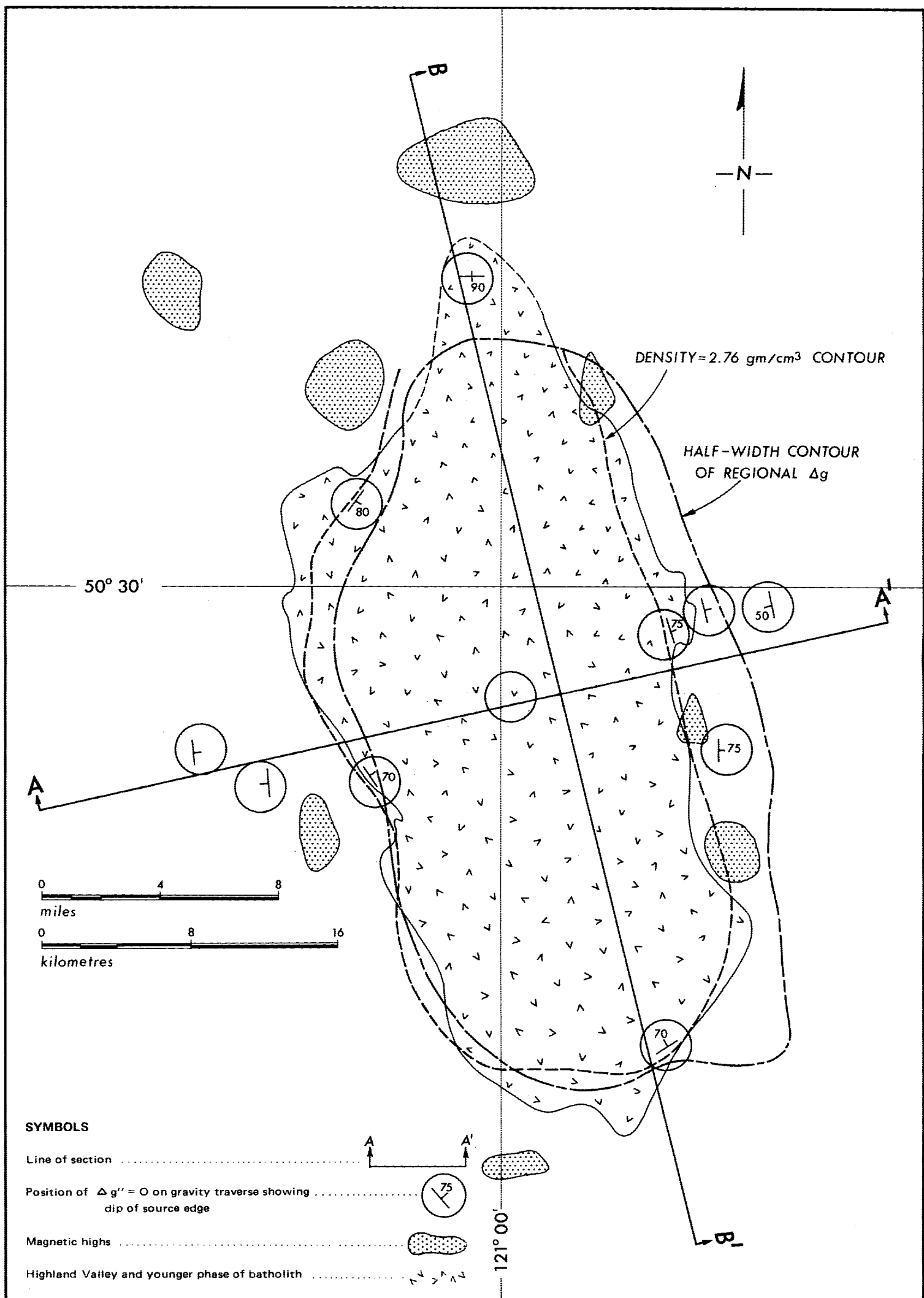


FIGURE 7.

COMPILATION OF GEOPHYSICAL DATA INDICATING DIPS ALONG THE
EDGE OF THE BATHOLITH.

FIGURE 8.

TOTAL AEROMAGNETIC FIELD MAP OF THE GUICHON CREEK BATHOLITH
DERIVED BY DIGITIZING PUBLISHED AEROMAGNETIC MAPS.

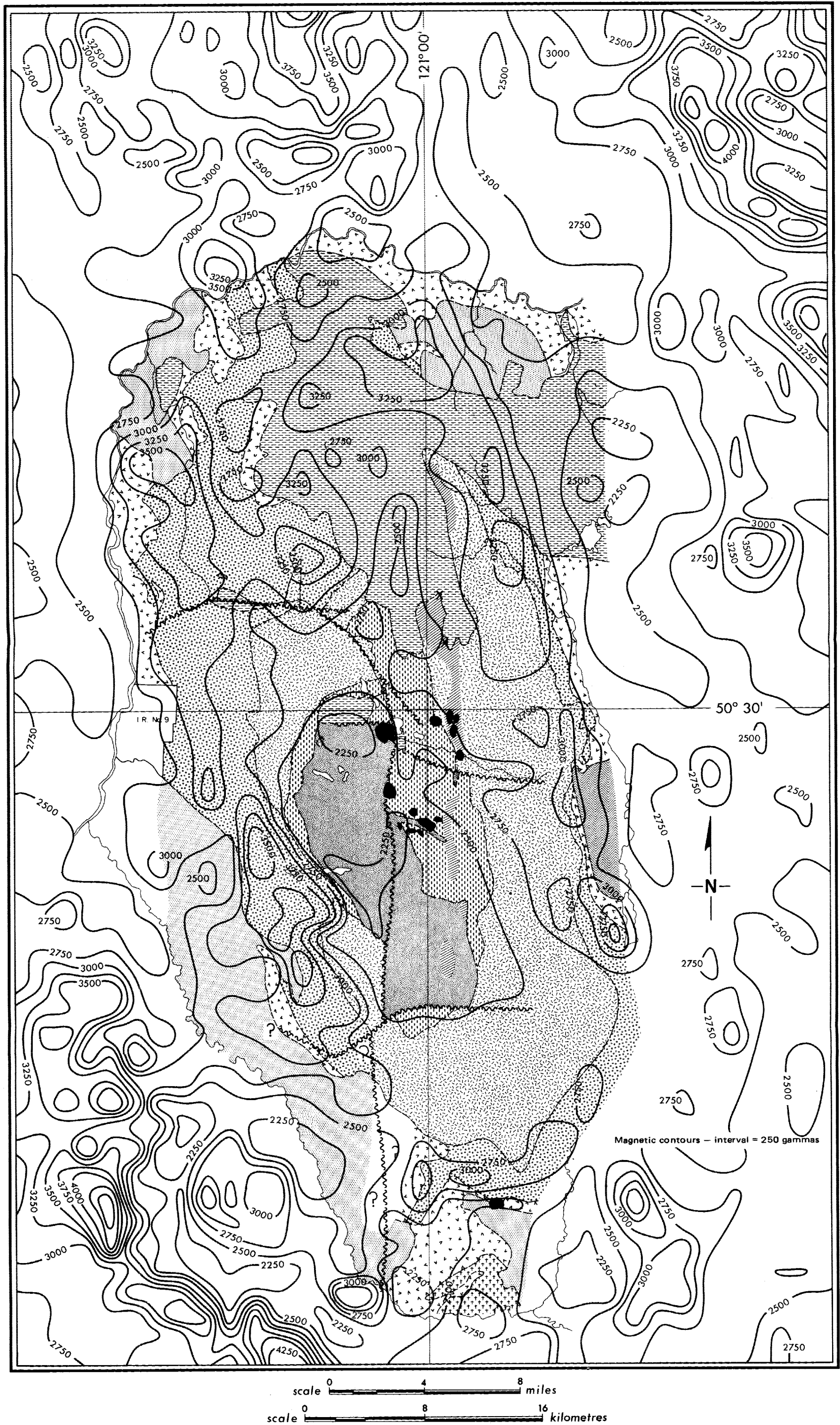


FIGURE 9.

REGIONAL AEROMAGNETIC MAP OF THE GUICHON CREEK BATHOLITH
DERIVED BY FILTERING THE TOTAL AEROMAGNETIC FIELD MAP.

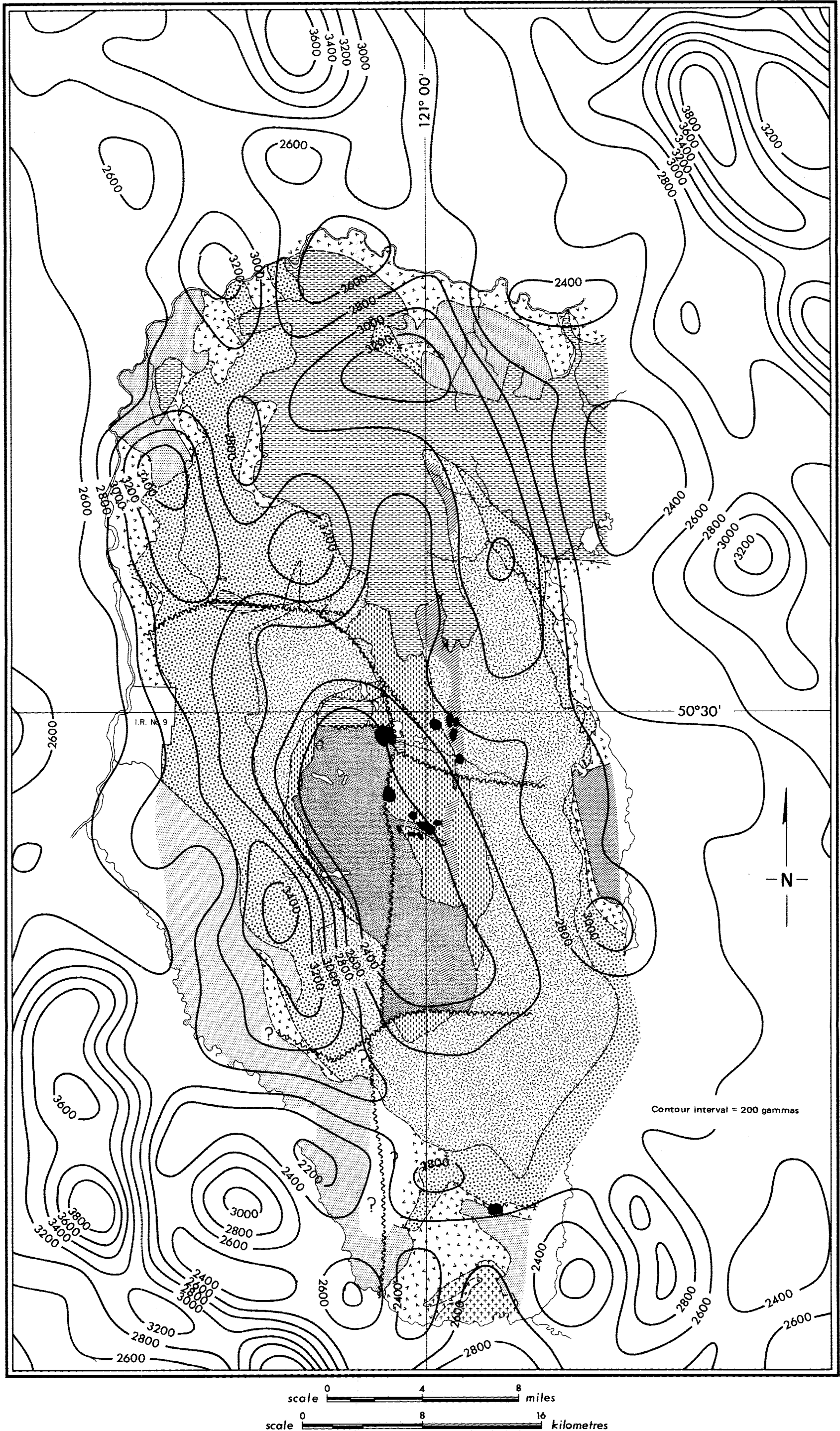
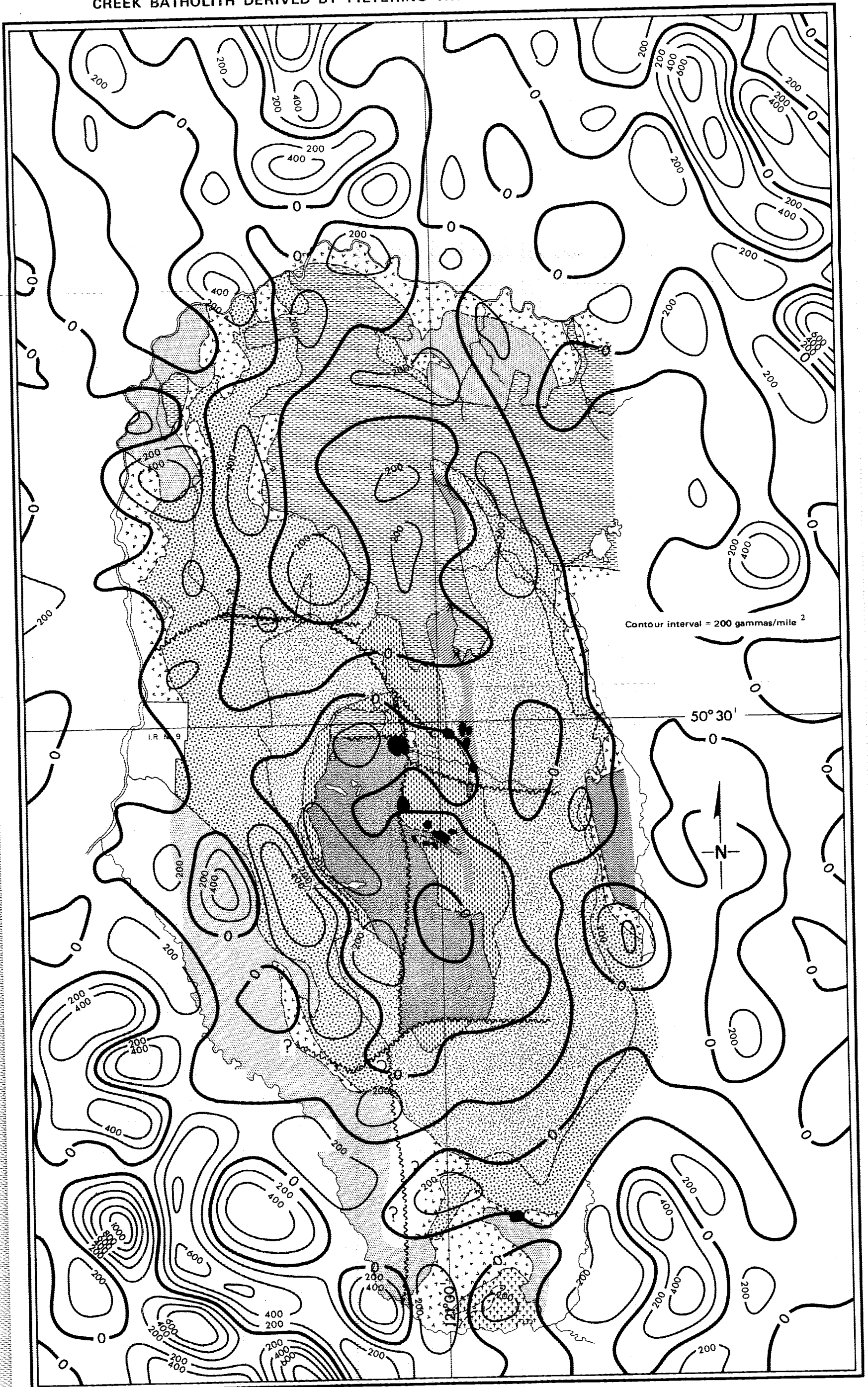


FIGURE 10.

SECOND VERTICAL DERIVATIVE AEROMAGNETIC MAP OF THE GUICHON CREEK BATHOLITH DERIVED BY FILTERING THE TOTAL AEROMAGNETIC FIELD MAP.



Contour interval = 200 gammas/mile²

50° 30'

scale 0 4 8 miles
scale 0 8 16 kilometres

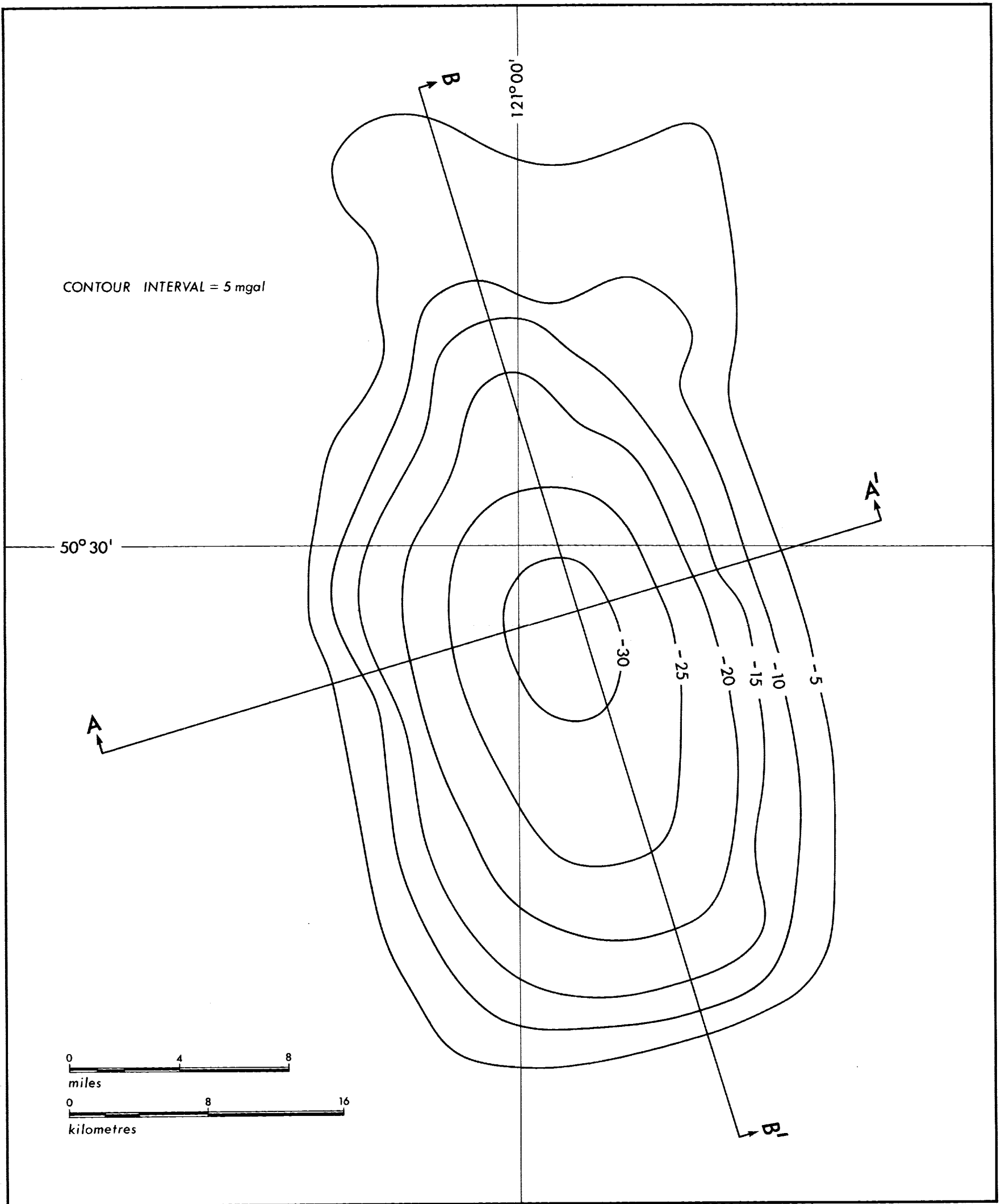


FIGURE 11(a).

CALCULATED GRAVITY MAP FOR MODEL OF THE GUICHON CREEK BATHOLITH.

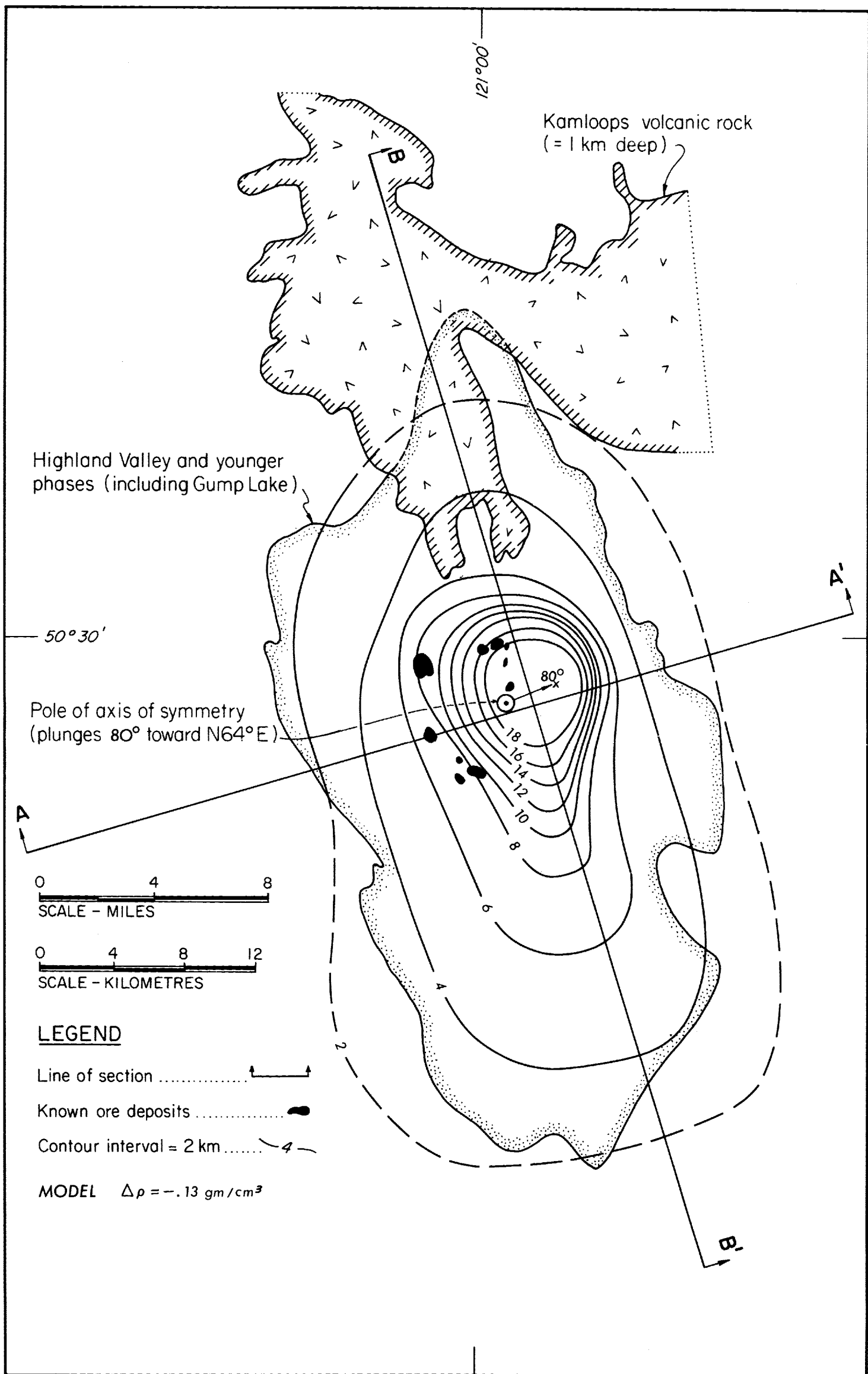


FIGURE 11(b).

GROSS SHAPE PLAN OF THE GUICHON CREEK BATHOLITH
DERIVED FROM THE GRAVITY DATA.

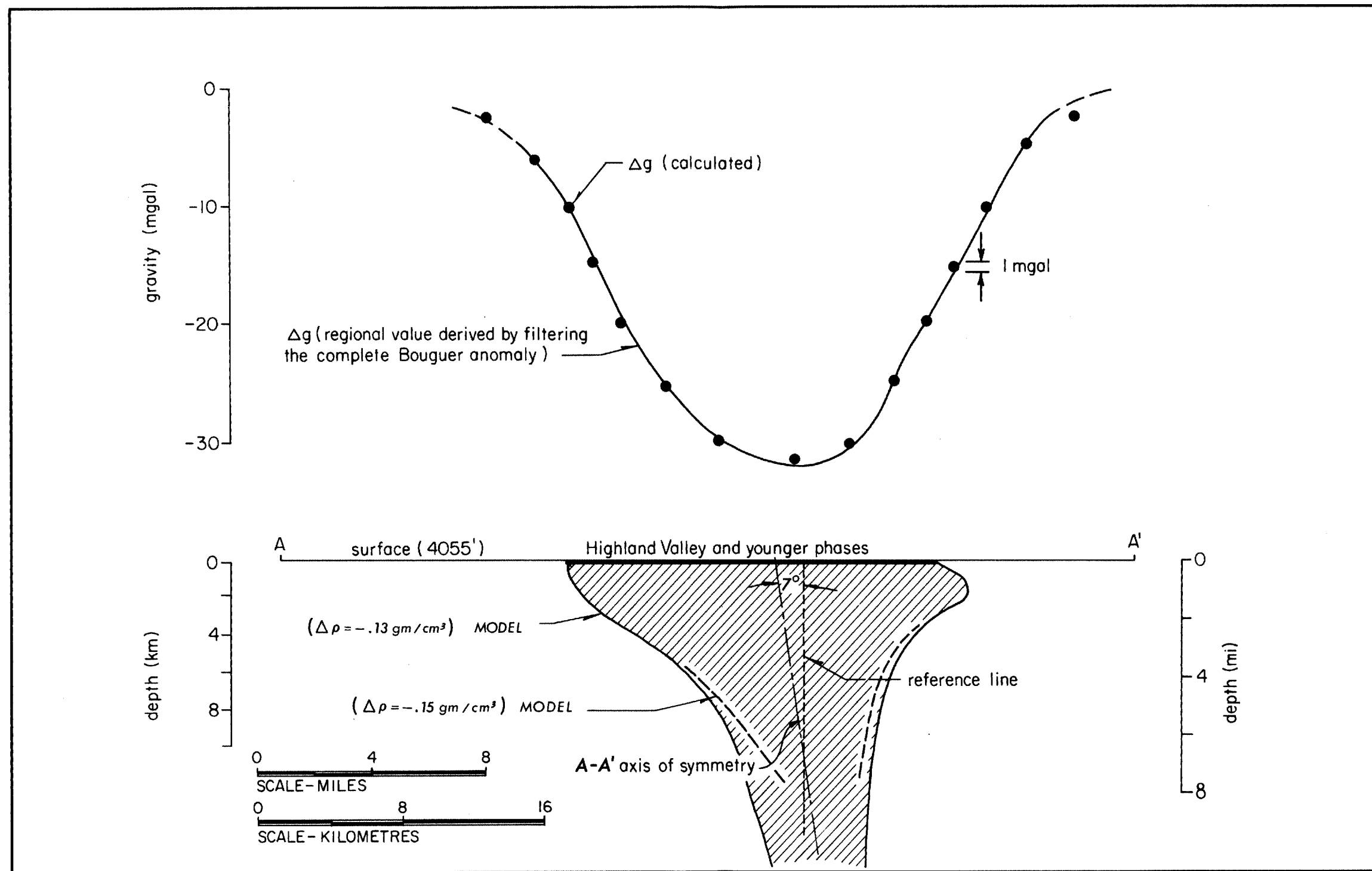


FIGURE 12.

DEPTH-GRAVITY SECTION A-A', LOOKING NORTHERLY.

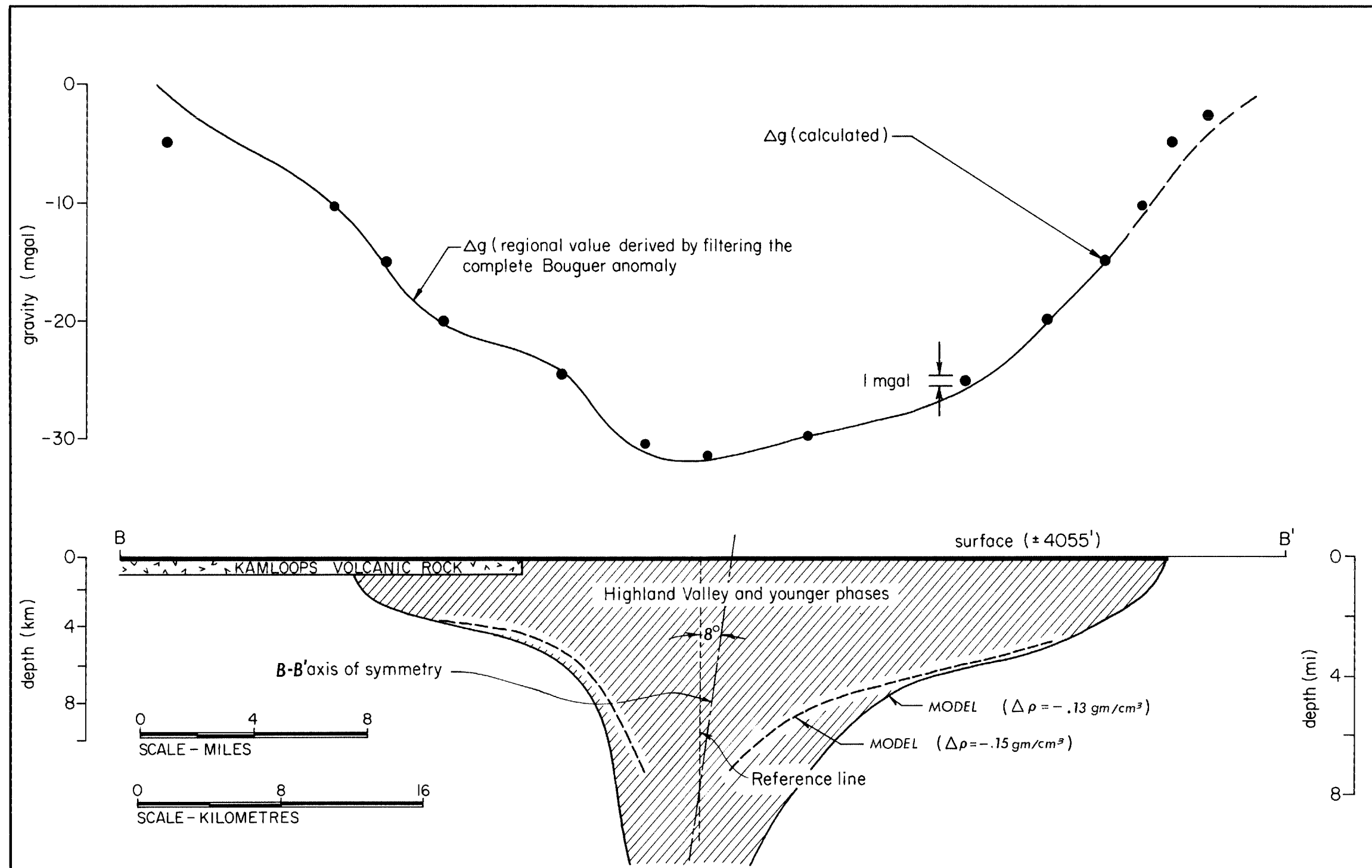


FIGURE 13.
DEPTH - GRAVITY SECTION B-B', LOOKING EASTERLY.